LETTER

doi:10.1038/nature11615

Controlled-reflectance surfaces with film-coupled colloidal nanoantennas

Antoine Moreau[1,2,3], Cristian Ciracì[1], Jack J. Mock[1], Ryan T. Hill[4], Qiang Wang[5,6], Benjamin J. Wiley[5], Ashutosh Chilkoti[4,7] & David R. Smith[1]

Efficient and tunable absorption is essential for a variety of applications, such as designing controlled-emissivity surfaces for thermophotovoltaic devices[1], tailoring an infrared spectrum for controlled thermal dissipation[2] and producing detector elements for imaging[3]. Metamaterials based on metallic elements are particularly efficient as absorbing media, because both the electrical and the magnetic properties of a metamaterial can be tuned by structured design[4]. So far, metamaterial absorbers in the infrared or visible range have been fabricated using lithographically patterned metallic structures[2,5–9], making them inherently difficult to produce over large areas and hence reducing their applicability. Here we demonstrate a simple method to create a metamaterial absorber by randomly adsorbing chemically synthesized silver nanocubes onto a nanoscale-thick polymer spacer layer on a gold film, making no effort to control the spatial arrangement of the cubes on the film. We show that the film-coupled nanocubes provide a reflectance spectrum that can be tailored by varying the geometry (the size of the cubes and/or the thickness of the spacer). Each nanocube is the optical analogue of a grounded patch antenna, with a nearly identical local field structure that is modified by the plasmonic response of the metal's dielectric function, and with an anomalously large absorption efficiency that can be partly attributed to an interferometric effect[10]. The absorptivity of large surface areas can be controlled using this method, at scales out of reach of lithographic approaches (such as electron-beam lithography) that are otherwise required to manipulate matter on the nanoscale.

To enhance the light absorbed within a medium, both the reflectance and the transmittance of the medium must be minimized. Although any opaque material, such as a metal, can essentially eliminate transmittance, eliminating the reflectance is more difficult. For a material defined by its electric permittivity, ε, and magnetic permeability, μ, the Fresnel reflection coefficient for the s polarization has the form

$$r_s = \frac{z_2\cos(\theta_i) - z_1\cos(\theta_t)}{z_2\cos(\theta_i) + z_1\cos(\theta_t)} \quad (1)$$

where $z_j = \sqrt{\mu_j/\varepsilon_j}$ is the wave impedance for material j, and θ_i and θ_t are the incident and transmitted angle of the wave with respect to the surface normal. For normal incidence, for which $\theta_i = \theta_t = 0$, equation (1) shows that if $z_1 = z_2$ then reflection is eliminated. In particular, for normal incidence any medium whose wave impedance has the vacuum value, $z_0 = \sqrt{\mu_0/\varepsilon_0}$, will be reflectionless in the vacuum. An opaque, impedance-matched structure can be considered an ideal absorber, because all incident light (at least that incident normally) must be absorbed.

Because magnetic response is far more limited in naturally occurring materials than in metamaterials, especially beyond frequencies of a few terahertz, impedance-matching a medium by introducing higher permeability materials is not generally feasible. In contrast, artificially structured metamaterials can have controlled magnetic as well as controlled electric properties at nearly any wavelength in the electromagnetic spectrum[11] (including the visible); metamaterials have thus been suggested as ideal absorbers[4]. It has been shown that a metamaterial composite comprising lithographically patterned resonant conducting elements on top of a conducting back plane can be made reflectionless for light incident over a broad range of angles[2,12]. To achieve the requisite magnetic response at infrared and visible wavelengths, a variety of metallic metamaterial structures have been used, such as cut-wire pairs[13,14]. By combining different types of metamaterial elements together into a single composite, more complicated reflectance spectra can be engineered, achieving the level of control needed in certain spectroscopy and energy-harvesting applications[7,12].

Because an absorbing structure does not require any substantial volume, the appropriateness of defining bulk constitutive parameters, such as ε and μ, which are rigorously defined only over a volume, can be called into question; thus, alternative descriptions have been proposed[8]. Here we similarly find it instructive to adopt a related model of reflection (Fig. 1). We view the metamaterial surface, or metasurface[15–17], as supporting both electric as well as fictitious magnetic surface current densities that are excited by the incident wave. Because both currents produce reflected waves that are exactly out of phase with each other, their sum can cancel out entirely if the total induced effective magnetic current exactly balances the total induced electric current[17].

Although magnetic conductors do not physically exist, many devices are commonly said to scatter waves via the excitation of effective magnetic currents. One example is that of the grounded patch antenna, which consists of a conducting metallic patch positioned above a conducting (ground) plane (Fig. 1e). The patch antenna supports a series of cavity-like resonances in which the electromagnetic field is localized within the gap between the ground plane and the patch element. For modes in which the electric field is maximum at the patch edges, the patch can be equivalently described as having a magnetic surface current density, K_M, that flows along the periphery of the patch, with magnitude given by $2E \times n$, where the field is determined at the patch edge and n is a unit vector normal to the surface. Thus, adding a population of patch antennas at some critical density to an otherwise conducting sheet can generate enough fictitious magnetic surface current density to offset the electric surface current density of an incident wave.

The underlying mode description of the patch is extensible to any wavelength as long as the patch and surface behave as conductors. Although metals are often described as lossy dielectric materials at optical wavelengths, they nevertheless support currents and can be used to form the optical equivalent of patch antennas[18]. We note that the particular arrangement of antennas on the surface should not matter for an isotropic absorber, because it is necessary to introduce only enough magnetic current to offset the electric current. Thus, an

[1]Center for Metamaterials and Integrated Plasmonics, Duke University, Durham, North Carolina 27708, USA. [2]Clermont Université, Université Blaise Pascal, Institut Pascal, BP 10448, 63000 Clermont-Ferrand, France. [3]CNRS, UMR 6602, IP, 63171 Aubière, France. [4]Center for Biologically Inspired Materials and Material Systems, Duke University, Durham, North Carolina, 27708, USA. [5]Department of Chemistry, Duke University, Durham, North Carolina 27708, USA. [6]Laboratory for Micro-sized Functional Materials & College of Elementary Education, Capital Normal University, Beijing 100048, China. [7]Department of Biomedical Engineering, Duke University, Durham, North Carolina 27708, USA.

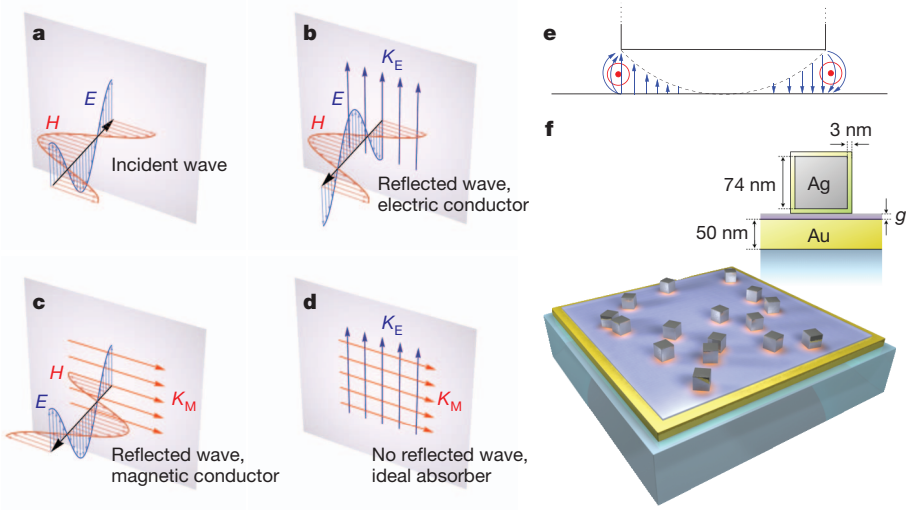

Figure 1 | Forming an ideal absorber. **a**–**d**, Light incident on a conductor (**a**) reflects due to either the excitation of electric surface current densities, K_E (**b**), or fictitious magnetic surface current densities, K_M (**c**). If both are excited then the back reflected wave represents the sum of the waves in **b** and **c**, for which the electric field, *E*, and the magnetic field, *H*, can exactly cancel, leaving the current to be absorbed (**d**). **e**, **f**, An ideal absorber can be formed by adding resonant nanoantennas a distance *g* above a conducting film (**f**), for which the enhanced electric field (blue) is equivalent to effective magnetic currents (red) (**e**).

artificially structured ideal absorber should not be reliant on any sort of patterning methods, and we can make use of colloidal self-assembly processes to very simply produce a randomized patch antenna geometry.

In plasmonic systems, field localization is generally correlated with local field enhancement, $f = E_l/E_0$, where E_l is the local electric field and E_0 is the electric field of the incident wave. In the present context, the enhancement serves to increase the effective magnetic surface current that flows in response to the applied field. Equivalently, the resonance can be viewed as enhancing the coupling between the gap modes and the incident field, enabling the incident fields to penetrate the gap region. In the latter interpretation, the enhanced absorption in the nanocube system can be considered to be closely related to the enhanced transmission in very thin slit arrays[19] and the large absorption that can be obtained with extremely shallow metallic gratings[20].

As a means of demonstrating the proposed colloidal approach to an ideal optical absorber, we consider nanocubes, with edge length ℓ, separated by a nanoscale distance from a gold film by a dielectric spacer layer with a refractive index of 1.54. To estimate the absorption efficiency of the nanoantennas, we perform numerical simulations over a domain containing a single absorber, and apply either periodic (Fourier modal method[21]) or absorbing (COMSOL) boundary conditions. As has been noted previously, square patches have scattering behaviour very similar to that of strips[8] because they share the same underlying mechanisms[7,18]; we are thus able to run two-dimensional simulations in many cases to perform quick optimizations, followed by fewer confirmative three-dimensional simulations.

A gap-plasmon guided mode, whose profile is shown Fig. 2, is supported under the cube. The constructive interferences of this mode, reflected back and forth at the edges of the cube, create a cavity resonance as in a Fabry–Pérot interferometer. This mechanism makes the resonance insensitive to the angle of incidence as well as to the polarization of the incident wave (see Supplementary Information for a detailed analysis).

When the thickness of the spacer layer is decreased, the effective index, n_e, of the mode increases, and can reach arbitrarily large values. Because the relation between the resonance wavelength and the cavity size, ℓ, is roughly $\ell \approx \lambda/2n_e$, resonances can thus be excited under cubes for which ℓ is only one-tenth of the wavelength, especially for very thin spacer layers. Figure 2 shows that the effective absorption efficiency, which is defined as the power absorbed by the nanocube divided by the incident intensity and normalized with respect to the actual surface occupied by a cube, is maximum for a spacer layer that is between 5 and 10 nm thick. For thicker spacer layers, the resonance is not as well formed, the reflection coefficient of the mode being relatively low. For extremely thin layers, the resonance is poorly excited by the incident field. The effective absorption efficiency can be as large as 30, meaning that in theory around 3% of the surface needs to be covered with cubes to reach almost complete absorption (Fig. 2).

Because the cavity is excited uniformly on both sides of the cube at normal incidence, it constitutes a perfect example of interferometrically controlled absorption[10]: the field amplitude is twice as large as if the cavity was excited from one side only, and the absorption is thus four times larger (especially compared with a structure like the shallow grating described in ref. 20, where the absorption mechanism is very similar). This phenomenon contributes to the very large absorption efficiency and explains why second-order resonances are not likely to be excited (Supplementary Information).

Having evaluated the underlying mechanisms of the nanoparticle-based ideal absorber, we next seek to implement the concept experimentally using chemically synthesized metal nanocubes that are randomly

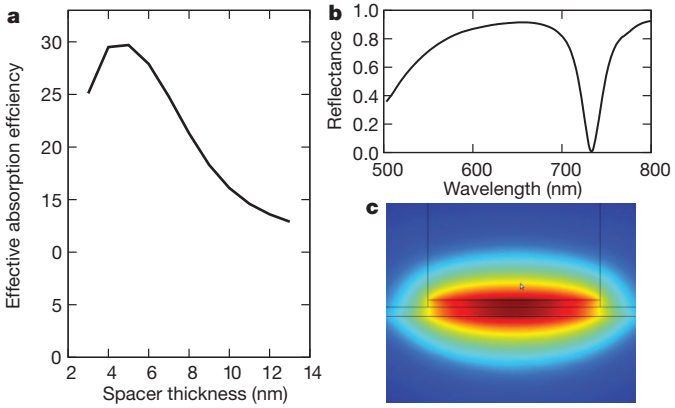

Figure 2 | Theoretical absorption efficiency of the nanocubes. **a**, Effective absorption efficiency as a function of the spacer thickness, defined as the ratio of the absorption cross-section to the physical cross-section for a single nanocube. The absorption cross-section is computed as the ratio of the energy absorbed to the illumination intensity. **b**, Reflectance spectrum for cubes that are 70 nm in size, periodically (350 nm) distributed and separated from the metallic film by a 8-nm-thick dielectric layer. **c**, Modulus of the magnetic field (red, high values; blue, low values) for the mode that is guided under the cube (out-of-plane wavevector). Black lines show the edges of the different materials in the COMSOL simulation.

adsorbed on an organic insulating spacer layer (of precisely controlled thickness) above a gold film. Because the synthetic chemistry for nanocubes favours silver rather than gold, we synthesized silver nanocubes with an edge length of 74 nm according to previously published protocols[22,23]. Electron microscopy images of the cubes are shown in Fig. 3. We note that a periodic arrangement of nanocubes would entirely suppress scattering, which is not the case for the random distributions considered here. Substantial scattering can thus be expected to occur from the nanoantennas, as confirmed by the dark-field optical images shown in Fig. 3c. The scattering places an upper limit on the reflectivity away from the absorption dip, as well as a lower limit on the reflectivity at the peak absorption.

Reflectance spectra were obtained from samples where 4.2% of the surface of the gold film was occupied by nanocubes and the nanocube–film separation distance was modulated by polyelectrolyte molecular spacer layers of increasing thicknesses[24–28]. Figure 4a shows the position of the measured resonance as a function of the overall thickness under the cubes, assuming that the nanocube–film separation distance is the sum of the polyelectrolyte spacer layer thickness and the 3-nm thickness of the stabilizer coating that surrounds the cubes. The position of the resonances can be accurately determined by three-dimensional simulations[21] if the coating and the rounded corners of the cubes are taken into account (by using a somewhat smaller cube dimension of 62 nm). Again, as is typical with nanoplasmonic systems, the resonance properties are crucially sensitive to the thickness and dielectric properties of the spacer layer, making the reflectance properties of the surface easily tunable by slightly changing the gap dimension.

On the basis of our three-dimensional simulations, which used a perfectly uniform population of cubes, we would expect a small reflectance even for such low surface coverage. However, the silver cubes as prepared varied in size. This variation contributes to a broader and shallower absorption dip in the reflectance. To achieve very low reflectance (without preparing a more uniform population of silver nanocubes), the concentration of cubes on the surface had to be increased. Figure 4b shows the relative reflectance observed from two nanocube–film samples. For one of them the surface coverage with imperfect cubes was 7.3%, and for the other it was 17.1%. For both, the nanocubes were separated from the gold film by a 6-nm polyelectrolyte layer. Figure 4b also shows the simulated reflectance for both perfectly uniform cubes and cubes with a size distribution similar to the experimental one. A reflectance of less than 7% is observed for normal incidence at 637 nm from samples with 17.1% surface coverage, further demonstrating the ease and extent to which the reflectance can be controlled.

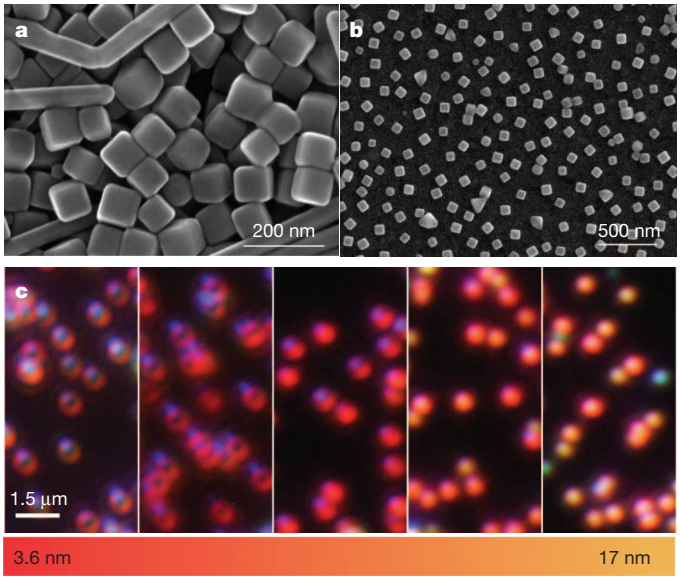

Figure 3 | Silver nanocubes. **a**, **b**, Scanning electronic microscopy images of the silver nanocubes as fabricated (**a**) and after deposition on the gold film with 17.1% surface coverage and remarkably uniform spacing (**b**). **c**, Dark-field images of the nanocubes randomly adsorbed on a nanoscale polymer spacer on a gold film, showing the light scattered by the individual nanocubes for less than 1% surface coverage. The spacer ranges in thickness from 3.6 to 17 nm.

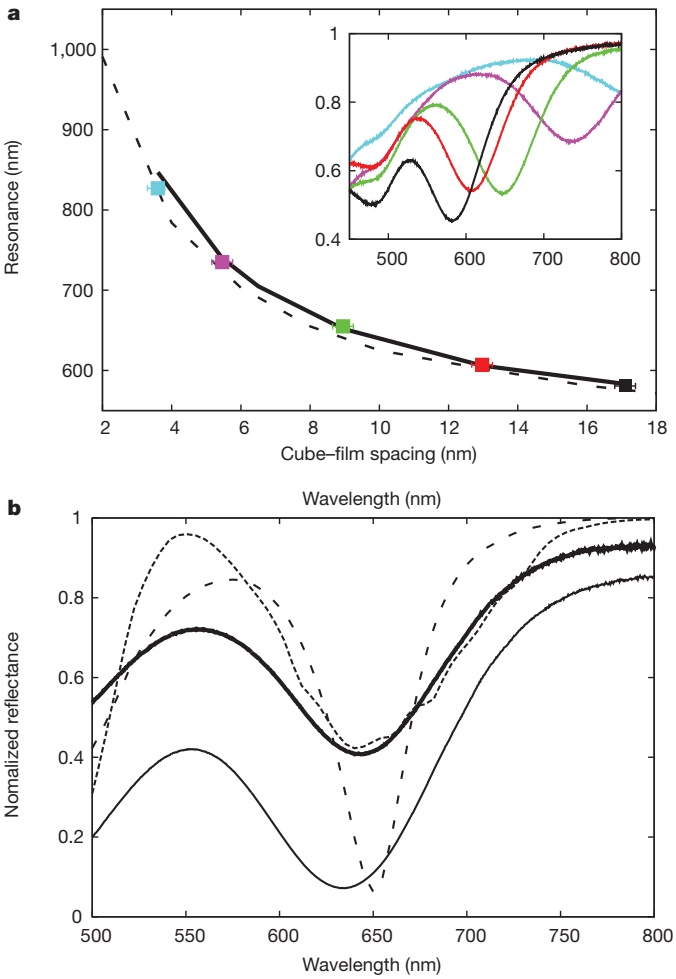

Figure 4 | Tunability of the reflectance. **a**, Position of the resonance as a function of the spacer thickness. Measured positions (black squares) for a cube surface density of 4.18% agree with three-dimensional simulations (solid line) and two dimensional simulations (dotted line) for 74-nm-wide gold nanorods surrounded by air. Inset, corresponding experimental reflectances for an angle of incidence of 25° and for the different spacer thicknesses. **b**, Experimental reflectance for normal incidence, normalized to the gold film, for surface coverages of 7.3% (thin solid line) and 17.1% (thick solid line), compared with simulations of uniform cubes (4.2% surface coverage, dotted line) and a model including size dispersion (dashed line; see Supplementary Information).

For many applications, a narrow absorption band may be desirable. Size dispersion seems to be the primary limitation on achieving much narrower spectroscopic features. This limitation can probably be overcome by using either fabrication processes that allow greater control or nanoparticle separation techniques[29,30]. The very small size and highly efficient optical response of the cubes suggests that mixed cube populations with controlled sized dispersion could be used further to tailor the absorption at will. Although those structures can be designed to operate in the infrared, we predict the introduction of alternative materials that would have better thermal properties. It is, however, worth underscoring that the extreme sensitivity of the resonant modes supported by the nanocubes can be exploited for immediate biosensor applications[30]. The gap-dependent cavity resonances have a completely different character from the classical resonances of spherical nanoparticles coupled to a film[28], so that in addition to their higher sensitivity, they can be excited very conveniently for normal incidence.

The spectral control available from absorbing metasurfaces forms the basis for a growing number of promising applications, including thermal detectors, light sources, energy-harvesting systems and even biosensors. Until now, structured absorbers have been successfully demonstrated across the entire electromagnetic spectrum, relying on top-down lithographic patterning as the fabrication approach. Although such patterning can produce highly uniform arrays of structures with high tolerances, it does not scale well to the large areas that will probably be needed in most applications of interest. By contrast, the bottom-up, colloidal approach described here is simple, rapid, inexpensive and easily scalable, and could lead to the eventual cost-effective manufacture of large-area metasurfaces with controlled reflectance.

METHODS SUMMARY

A 5-nm chromium adhesion layer and a 50-nm gold film were deposited by electron-beam evaporation onto a Nexterion Glass B slide. The surface of the gold film was then treated with a layer-by-layer deposition[24] of polyallylamine hydrochloride and polystyrene sulphonate to create a polyelectrolyte spacer layer with a controllable thickness[28]. The thickness of the polyelectrolyte layer was measured before deposition of the nanocubes using a J. A. Woolam Co. M-88 spectroscopic ellipsometer. The silver nanocubes were immobilized on the polyelectrolyte surface by a brief exposure to the colloidal solution followed by rinsing with water and drying under a stream of nitrogen. In an effort to limit the number of aggregates accumulating on the surface of the film, the exposure to the colloidal solution was carried out with the gold film facing down so that in theory aggregates would sink away from the surface. The nanocube coverage density on the gold film was controlled by varying the concentration of colloids in solution and the time that the surface was exposed to the solution. Scanning electron microscope images were used to determine the surface density of the cubes and their size distribution, which was found to have a standard deviation of the order of 10 nm (Supplementary Information). To measure the normal-incidence reflectance properties of the samples, white light from a 75-W xenon source was directed at the sample through a microscope objective with a numerical aperture of 0.13 and $\times 5$ magnification, and the reflected signal was collected by the same objective and directed though a 50/50 beam splitter to a spectrometer. For off-normal specular reflectance, 1-mm-diameter multimode fibres terminated with collimating lens adapters formed both the excitation path (from the light source to the sample) and the collection path (of the reflected signal from the sample to the spectrometer).

Full Methods and any associated references are available in the online version of the paper.

Received 18 April; accepted 24 September 2012.

1. Bermel, P. *et al.* Design and global optimization of high-efficiency thermophotovoltaic systems. *Opt. Express* **18,** A314–A334 (2010).
2. Hao, J. *et al.* High performance optical absorber based on a plasmonic metamaterial. *Appl. Phys. Lett.* **96,** 251104 (2010).
3. Niesler, F., Gansel, J., Fischbach, S. & Wegener, M. Metamaterial metal-based bolometers. *Appl. Phys. Lett.* **100,** 203508 (2012).
4. Landy, N. I., Sajuyigbe, S., Mock, J. J., Smith, D. R. & Padilla, W. J. Perfect metamaterial absorber. *Phys. Rev. Lett.* **100,** 207402 (2008).
5. Avitzour, Y., Urzhumov, Y. A. & Shvets, G. Wide-angle infrared absorber based on a negative-index plasmonic metamaterial. *Phys. Rev. B* **79,** 045131 (2009).
6. Liu, N., Mesch, M., Weiss, T., Hentschel, M. & Giessen, H. Infrared perfect absorber and its application as plasmonic sensor. *Nano Lett.* **10,** 2342–2348 (2010).
7. Koechlin, C. *et al.* Total routing and absorption of photons in dual color plasmonic antennas. *Appl. Phys. Lett.* **99,** 241104 (2011).
8. Wu, C. *et al.* Large-area wide-angle spectrally selective plasmonic absorber. *Phys. Rev. B* **84,** 075102 (2011).
9. Tittl, A., Mai, P., Taubert, R., Dregely, D. & Giessen, N. L. H. Palladium-based plasmonic perfect absorber in the visible wavelength range and its application to hydrogen sensing. *Nano Lett.* **11,** 4366–4369 (2011).
10. Wan, W. *et al.* Time-reversed lasing and interferometric control of absorption. *Science* **331,** 889–892 (2011).
11. Shalaev, V. Optical negative-index metamaterials. *Nature Photon.* **1,** 41–48 (2007).
12. Liu, X. *et al.* Taming the blackbody with infrared metamaterials as selective thermal emitters. *Phys. Rev. Lett.* **107,** 045901 (2011).
13. Dolling, G. *et al.* Cut-wire pairs and plate pairs as magnetic atoms for optical metamaterials. *Opt. Lett.* **30,** 3198–3200 (2005).
14. Shalaev, V. M. *et al.* Negative index of refraction in optical metamaterials. *Opt. Lett.* **30,** 3356–3358 (2005).
15. Yu, N. *et al.* Light propagation with phase discontinuities: generalized laws of reflection and refraction. *Science* **334,** 333–337 (2011).
16. Shadrivov, I. V., Kapitanova, P., Maslovski, S. & Kivshar, Y. Metamaterials controlled with light. *Phys. Rev. Lett.* **109,** 083902 (2012).
17. Albooyeh, M. & Simovski, C. Maximal absorption and local field enhancement in planar plasmonic arrays. Preprint at http://arxiv.org/abs/1203.2100v1 (2012).
18. Bozhevolnyi, S. I. & Søndergaard, T. General properties of slow-plasmon resonant nanostructures: nano-antennas and resonators. *Opt. Express* **15,** 10869–10877 (2007).
19. Moreau, A., Lafarge, C., Laurent, N., Edee, K. & Granet, G. Enhanced transmission of slits arrays in an extremely thin metallic film. *J. Opt. A* **9,** 165–169 (2007).
20. Le Perchec, J., Quemerais, P., Barbara, A. & Lopez-Ros, T. Why metallic surfaces with grooves a few nanometers deep and wide may strongly absorb visible light. *Phys. Rev. Lett.* **100,** 066408 (2008).
21. Granet, G. & Plumey, J. Parametric formulation of the Fourier modal method for crossed surface-relief gratings. *J. Opt. A* **4,** S145 (2002).
22. Sun, Y. & Xia, Y. Shape-controlled synthesis of gold and silver nanoparticles. *Science* **298,** 2176–2179 (2002).
23. Im, S. H., Lee, Y. T., Wiley, B. & Xia, Y. Large-scale synthesis of silver nanocubes: the role of HCl in promoting cube perfection and monodispersity. *Angew. Chem. Int. Ed.* **44,** 2154–2195 (2005).
24. Decher, G. Fuzzy nanoassemblies: toward layered polymeric multicomposites. *Science* **277,** 1232–1237 (1997).
25. Marinakos, S. M., Chen, S. & Chilkoti, A. Plasmonic detection of a model analyte in serum by a gold nanorod sensor. *Anal. Chem.* **79,** 5278–5283 (2007).
26. Michota, A., Kudelski, A. & Bukowska, J. Molecular structure of cysteamine monolayers on silver and gold substrates: comparative studies by surface-enhanced Raman scattering. *Surf. Sci.* **502–503,** 214–218 (2002).
27. Wallwork, M. L., Smith, D. A., Zhang, J., Kirkham, J. & Robinson, C. Complex chemical force titration behavior of amine-terminated self-assembled monolayers. *Langmuir* **17,** 1126–1131 (2001).
28. Mock, J. J. *et al.* Distance-dependent plasmon resonant coupling between a gold nanoparticle and gold film. *Nano Lett.* **8,** 2245–2252 (2008).
29. Hanauer, M., Pierrat, S., Zins, I., Lotz, A. & Sönnichsen, C. Separation of nanoparticles by gel electrophoresis according to size and shape. *Nano Lett.* **7,** 2881–2885 (2007).
30. Anker, J. N. *et al.* Biosensing with plasmonic nanosensors. *Nature Mater.* **7,** 442–453 (2008).

Supplementary Information is available in the online version of the paper.

Acknowledgements This work was supported by the US Air Force Office of Scientific Research (grant no. FA9550-09-1-0562) and by the US Army Research Office through a Multidisciplinary University Research Initiative (grant no. W911NF-09-1-0539). Additional support includes US NIH grant R21EB009862, to A.C., and US NIH F32 award (F32EB009299), to R.T.H.

Author Contributions A.M. and C.C. ran the simulations. A.M., C.C., J.J.M. and D.R.S. conducted the physical analysis. Q.W. fabricated and characterized the nanocubes. R.T.H. made the substrates (gold and polyelectrolyte layers), measured their characteristics and deposited the cubes. J.J.M. built the experimental set-up and made the measurements. All the authors provided technical and scientific insight and contributed to the writing of the manuscript.

Author Information Reprints and permissions information is available at www.nature.com/reprints. The authors declare no competing financial interests. Readers are welcome to comment on the online version of the paper. Correspondence and requests for materials should be addressed to D.R.S. (drsmith@ee.duke.edu).

METHODS

A 50-nm-thick gold film was deposited by electron-beam evaporation (CHA Industries), at 2 Å s^{-1} onto a Nexterion Glass B slide (Schott North America, Inc.), including a 5-nm chromium adhesion layer (deposited at 1 Å s^{-1}).

The surface of the gold film was then treated by layer-by-layer deposition[24] of polyallylamine hydrochloride (Aldrich) and polystyrene sulphonate (Aldrich) to create a polyelectrolyte spacer layer with a controllable thickness[28]. For each deposition step, the gold-coated glass slides were immersed for 30 min in polyelectrolyte at a concentration of 0.003 moles of monomer per litre and 1 M NaCl, rinsed thoroughly with a gentle stream of ultrapure water (18 MΩ, used throughout) and immersed in fresh ultrapure water for 1 min, after which the substrates were either immersed in 1 M NaCl for 30 s before repeating the same steps for deposition of the oppositely charged polyelectrolyte or dried with a stream of high-purity nitrogen for analysis. All layer-by-layer depositions were initiated and terminated with the cationic polyallylamine hydrochloride layer to facilitate both the attachment of the first polyelectrolyte layer to the gold film through amine–gold interactions[25–27] and the electrostatic immobilization of the silver nanocubes.

The nanocubes, which were made following a previously published protocol[22], were immobilized on the polyelectrolyte surface by brief exposure to the colloidal solution followed by rinsing with water and drying under a stream of nitrogen. In an effort to limit the number of aggregates accumulating on the surface of the film during this attachment process, the nanocube solution was sonicated briefly and the slide was lowered gold side down onto a coverslip containing a 30-μl droplet of the colloidal solution, whereupon the coverslip was picked up by the slide using the capillary force of the droplet spreading onto the film surface. Under these conditions, aggregates would theoretically sink away from the surface of the gold film during the incubation. The density of coverage of nanocubes on the surface of the gold film was controlled by varying the concentration of colloids in solution and the time that the surface was exposed to the colloidal solution.

Scanning electronic microscope images were used to determine both the surface density of the cubes after deposition on the layers and the size distribution of the cubes. This distribution was found to have a standard deviation of the order of 10 nm (Supplementary Information). The thickness of the polyelectrolyte layer was measured before deposition of the nanocubes using a J. A. Woolam Co. M-88 spectroscopic ellipsometer.

To measure the normal-incidence specular reflectance properties of the samples, white light from a 75-W xenon source (ORIEL) was directed at the sample through a microscope objective with a numerical aperture of 0.13 and ×5 magnification (Nikon), and the reflected signal was collected by the same objective and directed though a 50/50 beam splitter to a spectrometer (ACTON 2300i). For off-normal (25°) specular reflectance, 1-mm-diameter multimode fibres terminated with collimating lens adapters formed both the excitation path (from the light source to the sample) and the collection path (of the reflected signal from the sample to the spectrometer). With this technique, the beam diameter at the surface of the sample is approximately 3 mm. In all of the presented data, the reflectivity of the cube-covered film is normalized by the reflectance spectrum of the bare gold film.